A crisis in the dissipative Fermi accelerator model

LETTER TO THE EDITOR

A crisis in the dissipative Fermi accelerator model

Edson D Leonel and P V E McClintock

Department of Physics, Lancaster University, Lancaster, LA1 4YB, UK

Abstract
The dynamics of the full, dissipative, Fermi accelerator model is shown to exhibit crisis events as the damping coefficient is varied. The investigation, based on analysis of a two-dimensional nonlinear map, has also led to a numerical determination of the basin of attraction for its chaotic attractor.

PACS numbers: 05.45.−a, 45.50.Dd

A major challenge in the investigation of nonlinear systems is that of explaining/predicting the often unexpected phenomena that they exhibit. A closely related goal is to characterize their dynamical properties. Chaotic behaviour appears quite frequently in such systems, both in the presence and the absence of dissipation [1–3]. For the dissipative case, the area-contracting property leads to time evolution of initial conditions towards a range of different asymptotic behaviours, e.g. fixed points, limit cycles (sometimes of high order) as well as chaotic attractors. There also exist systems with more than one chaotic attractor [4] where interest frequently centres on determination of the basins of attraction for each chaotic attractor, whose boundaries can be either continuous or fractal. Particular cases can also be observed where the asymptotic behaviour wanders in an erratic way but is not characterized by a positive Lyapunov exponent (the commonest tool for classification of the behaviour as chaotic) [5]. For the non-dissipative case, the characteristic structure of Hamiltonian systems is observed, often with a mixed phase space structure is commonly present in the sense that Kolmogorov–Arnol'd–Moser (KAM) islands exist, together with invariant spanning curves separating different portions of the phase space and chaotic seas [6–9]. The tools developed to study both the dissipative and non-dissipative cases are widely applicable in many different fields of physics, including astrophysics, plasma physics, fluids, accelerators and planetary motion.

In this letter, we revisit the classical problem of the bouncing ball, a model originally proposed by Enrico Fermi [10] in an attempt to describe the acceleration of cosmic rays. It provides a mechanism through which charged particles can be accelerated by collisions with moving magnetic field structures. The model was later modified and studied in different variants. The Fermi–Ulam approach [11] considers the dynamics of a classical particle bouncing between two rigid walls, one of which is fixed and the other moves in time. The main result for periodic oscillation is that the phase space presents KAM islands surrounded by a chaotic sea. Unlimited energy growth (i.e. the condition for observing Fermi acceleration)

is not, however, observed because the phase space exhibits a set of invariant spanning curves. An alternative version of this model proposed by Pustylnikov [12], often referred to as a bouncer [13], consists of a classical particle falling in a constant gravitational field, on a moving platform. Its most important property is that, in contradistinction to the Fermi–Ulam model, depending on both the initial conditions and control parameters, there could be no bound to the energy gained by the bouncing particle. The distinctive difference between the models was later clarified by Lichtenberg *et al* [14]. The corresponding quantum versions of both the bouncer and Fermi–Ulam models have also been studied [15–19]. Recently, we have proposed a hybrid version of these two models [20]. It considers the motion of a classical particle in a gravitational field, with the motion confined between two rigid walls, one of which is fixed while the other one moves in time. We showed that our model recovers the well-known Fermi–Ulam model results in the limit of zero external field and shows properties of the bouncer model for intense gravitational field. Within a certain range of control parameters, however, we found that properties that are individually characteristic of either the Fermi–Ulam or bouncer models can come together and coexist in their hybrid.

We now consider here a classical particle in the Fermi–Ulam model suffering an inelastic collision with the fixed wall, and we analyse the full model rather than the simplified system that is commonly considered where the so-called *successive collisions* are ignored (see [21–23] for previous results in the simplified and dissipative version of the model). We will show, however, that the model is area contracting only in relation to non-successive collision; in contrast, the map describing successive collisions retains the area-preserving property (because collisions with the moving wall are elastic in the moving frame of reference). We also show that dissipation destroys the mixed phase space structure seen in the non-dissipative case. We observe a chaotic attractor, characterized by a positive Lyapunov exponent and, of particular interest, we identify and characterize a crisis event [24, 25] for this version of the problem. In addition, the basin of attraction for the chaotic attractor is located and the manifold branches obtained.

The model thus consists of a classical particle confined to move between two rigid walls in the absence of gravitational or other fields. One wall is fixed at $x = l$ and the other moves according to the equation $x_w(t) = \epsilon' \cos(\omega t)$, where ϵ' and ω are, respectively, the amplitude and angular frequency of the motion. We assume that collisions with the moving wall are perfectly elastic in the frame of reference of the moving wall, but that those with the fixed wall are inelastic. In a collision with the fixed wall, the particle's velocity is inverted but, in addition, it is also reduced by a factor depending on the coefficient of restitution α which assumes a value in the interval $\alpha \in [0, 1]$: $\alpha = 1$, corresponding to perfect elasticity, obviously leads to recovery of all the results of the non-dissipative case; $\alpha = 0$ corresponds to the completely inelastic case where a single collision with the wall is enough to terminate the particle's dynamics. Our interest relates to cases lying between these two limits.

In constructing a map to describe the dynamics of this model, it is convenient to use dimensionless variables. We define that $V_n = v_n/(\omega l)$, $\epsilon = \epsilon'/l$ and measure time in terms of the number of oscillations of the moving wall, i.e. $\phi_n = \omega t$. Starting with the initial conditions (V_n, ϕ_n), with the particle's initial position given by $x_p(\phi_n) = \epsilon \cos(\phi_n)$, the map describing the model dynamics is

$$T : \begin{cases} V_{n+1} = V_n^* - 2\epsilon \sin(\phi_{n+1}) \\ \phi_{n+1} = \phi_n + \Delta T_n \, \text{mod}(2\pi) \end{cases}$$

where the expressions to be used for V_n^* and ΔT_n depend on which kind of collision occurs. For successive collisions, the expressions are $V_n^* = -V_n$ and $\Delta T_n = \phi_c$. The phase ϕ_c is obtained as the smallest solution of the equation $G(\phi_c) = 0$ for $\phi_c \in (0, 2\pi]$. The physical

interpretation of $G(\phi_c) = 0$ is equivalent to having the condition $x_p = x_w$, i.e. the position of the particle is the same as the position of the moving wall, which obviously corresponds to a collision. The function $G(\phi)$ is given by

$$G(\phi) = \epsilon \cos(\phi_n + \phi) - \epsilon \cos(\phi_n) - V_n \phi. \tag{1}$$

If the function $G(\phi)$ does not have a root in the interval $\phi \in (0, 2\pi]$, thus we can conclude that the particle leaves the collision zone without suffering a successive collision. The collision zone is defined as the interval $x \in [-\epsilon, \epsilon]$. The Jacobian matrix for successive collisions yields a determinant given by

$$\text{Det } J = \frac{V_n + \epsilon \sin(\phi_n)}{V_{n+1} + \epsilon \sin(\phi_{n+1})}.$$

This result shows that the mapping preserves the measure of phase space $d\mu = (V + \epsilon \sin(\phi)) \, dV \, d\phi$; it is the same as the measure obtained for the breathing circle billiard [26]. Note that the results for a diametrical orbit in such a billiard necessarily recovers the results of the Fermi–Ulam model itself. For the case of non-successive collisions, the expressions are given by $V_n^* = \alpha V_n$ and $\Delta T_n = \phi_r + \phi_l + \phi_c$ where the auxiliary terms take the form

$$\phi_r = \frac{1 - \epsilon \cos(\phi_n)}{V_n}, \qquad \phi_l = \frac{1 - \epsilon}{\alpha V_n}.$$

The term ϕ_r indicates the time spent by the particle in travelling towards the fixed wall, while ϕ_l gives the time the particle spends before reaching the collision zone after suffering an inelastic collision with the fixed wall. Finally, the term ϕ_c is obtained numerically as the smallest solution of the equation $F(\phi_c) = 0$ where the function $F(\phi)$ is given by

$$F(\phi) = \epsilon \cos(\phi_n + \phi_r + \phi_l + \phi) - \epsilon + \alpha V_n \phi. \tag{2}$$

Equation (2) is obtained in the attempt to meet the condition $x_p = x_w$. The Jacobian matrix for this case yields the determinant

$$\text{Det } J = \alpha^2 \frac{V_n + \epsilon \sin(\phi_n)}{V_{n+1} + \epsilon \sin(\phi_{n+1})},$$

which obviously implies that area preservation is observed only if $\alpha = 1$.

The expression $-2\epsilon \sin(\phi_{n+1})$ (see the map T) is obtained by conservation of energy and momentum in the reference frame of the moving wall at the instant of impact, for which it is instantaneously at rest.

Figure 1 shows the stable and unstable manifolds for a hyperbolic fixed point (also called as saddle) given by

$$V = \frac{2\epsilon}{\alpha - 1} \sin(\phi), \qquad \phi = -\arccos\left[\frac{\epsilon - \beta\sqrt{\beta^2 + \epsilon^2 - 1}}{\epsilon^2 + \beta^2} \right] \tag{3}$$

with $\beta = 4\pi\epsilon\alpha/(\alpha^2 - 1)$ in this version of the dissipative Fermi–Ulam model. Figure 1(a) shows the results for $\alpha = 0.93$ and $\epsilon = 0.04$. The two branches of the unstable manifold evolve as follows: the upward branch generates the attracting fixed point while the downward branch generates the chaotic attractor. The two branches of the stable manifold establish boundaries for both the chaotic and fixed point attractors (the details of the corresponding basin boundaries are shown in figure 2(b)). Increasing the value of the control parameter α, which is equivalent to reducing the strength of the dissipation, causes a homoclinic orbit to be generated at $\alpha \approx 0.936\,24\ldots$. Since the two branches of the stable manifold establish the edges of the basin boundaries, the generation of the homoclinic orbit also results in a collision of the chaotic attractor with the border of its basin boundary. Such a collision is often called a
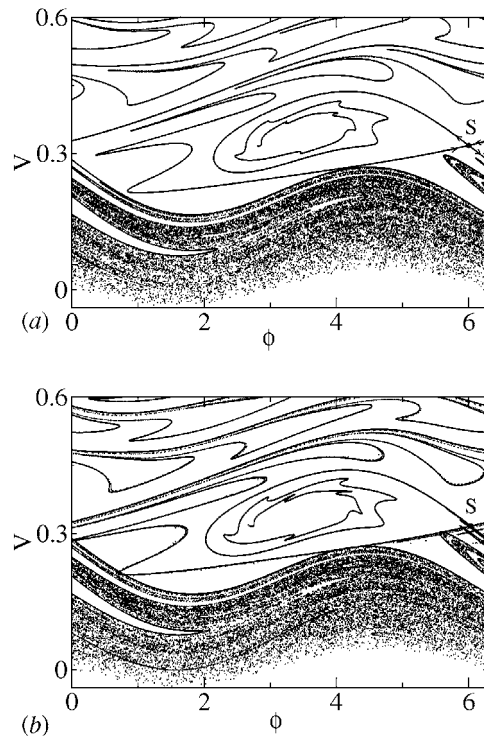
Figure 1. Stable and unstable manifolds for the dissipative Fermi–Ulam model with $\epsilon = 0.04$: (a) for $\alpha = 0.93$, just before the crisis and (b) for $\alpha = 0.9375$, just after the crisis. The saddle is indicated by an S. Note that in (b), unlike (a), the manifolds cross.

boundary crisis [24, 25, 27]. Simultaneously, the chaotic attractor and its basin of attraction are destroyed. Figure 1(b) shows the stable and unstable manifolds for the control parameters $\epsilon = 0.04$ and $\alpha = 0.9375$ immediately after the boundary crisis. The birth of the homoclinic orbit is clearly evident.

The chaotic attractor is shown in figure 2(a). The control parameters used in constructing the figure were $\epsilon = 0.04, \alpha = 0.936\,24$. The asymptotic positive Lyapunov exponent, obtained via a triangularization algorithm [28], is given by $\lambda = 1.7743 \pm 0.0005$. We used an ensemble of ten different initial conditions randomly chosen in the basin of attraction of the chaotic attractor. Each initial condition was evolved through up to 10^8 iterations. The error represents the standard deviation of the ten samples. It is interesting to note that the lower bound of the chaotic attractor has a simple physical interpretation. It is, in fact, limited by the velocity of the moving wall, i.e. $V_w = \mathrm{d}x_w/\mathrm{d}\phi = -\epsilon \sin(\phi)$: the line generated by V_w is shown in the figure. The attracting fixed point is indicated by a $\times$ in figure 2(a). The basins of attraction for both the chaotic and fixed point attractors are shown in figure 2(b) for the same parameters as used in figure 2(a). We set a range for the initial conditions as $V \in [-\epsilon, 0.6]$ and $\phi \in [0, 2\pi]$. We thus divide both windows of V and ϕ in 200 parts each, leading then to a total of 4×10^4 initial conditions. Each initial condition was iterated up to $n_x = 5 \times 10^5$ iterations, which is quite enough to disregard transient effects for the particular combination of control parameters used. The basins of attraction of the chaotic and fixed point attractors are shown in black and grey, respectively. The border of the boundary is obtained by iteration
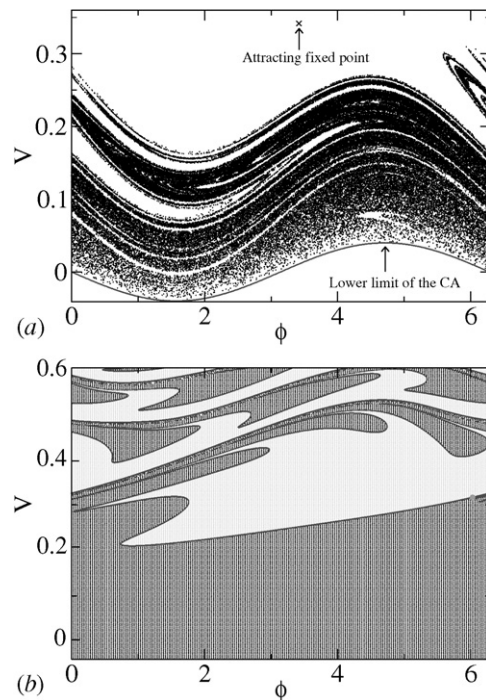
Figure 2. (*a*) The chaotic attractor and the coexisting attracting fixed point for the parameters $\epsilon = 0.04$ and $\alpha = 0.936\,24$. (*b*) Their corresponding basin boundaries. The basin boundary of the chaotic attractor is shown in black, while that of the attracting fixed point is in grey. The border was obtained as the stable manifolds of the fixed point given by equation (3).

of the stable manifolds of the fixed point given by equation (3). Immediately after the birth of the homoclinic orbit, and the destruction of the chaotic attractor and its basin, some initial conditions may lead to very long transients before the attracting fixed point is reached, even compared to $n_x = 5 \times 10^5$. For such initial conditions, we therefore extend the simulation to $n_x = 1 \times 10^7$ or longer in order to guarantee convergence to the attracting fixed point. Other periodic attracting orbits could in principle also exist in this version of the model. We therefore stress that for the control parameters used in figure 2, for the range of V and ϕ considered and for the steps used in the basin boundary construction, no such orbits were observed: if they exist their basins of attraction must be very small.

In summary, we have studied a dissipative version of the well-known Fermi–Ulam model. It considers inelastic collisions with the fixed wall while assuming elastic collisions with the moving wall. We find that, depending on the type of collision, the mapping may show either area preservation or area contraction. We show that crisis events arise as a function of the magnitude of the coefficient of restitution. Basin boundaries were obtained for both the chaotic and fixed point attractors.

Acknowledgments

References

[1] Lichtenberg A J and Lieberman M A 1992 *Regular and Chaotic Dynamics, Applied Mathematical Sciences* vol 38 (New York: Springer)

[2] Bai-Lin H 1990 *Chaos II* (Singapore: World Scientific)

[3] Guckenheimer J and Holmes P 2000 *Nonlinear Oscillations, Dynamical Systems, and Bifurcations of Vector Fields, Applied Mathematical Sciences* vol 42 (New York: Springer)

[4] Nusse H E and Yorke J A 1991 *DYNAMICS: Numerical Explorations, Applied Mathematical Sciences* vol 101 (New York: Springer)

[5] Grebogi C, Ott E, Pelikan S and Yorke J A 1984 *Physica* D **13** 261

[6] Leonel E D and da Silva J K L 2003 *Physica* A **323** 181

[7] Leonel E D, da Silva J K L and Kamphorst S O 2004 *Physica* A **331** 435

[8] Leonel E D and McClintock P V E 2004 *J. Phys. A: Math. Gen.* **37** 8949

[9] Leonel E D and McClintock P V E 2004 *Phys. Rev.* E **70** 016214

[10] Fermi E 1949 *Phys. Rev.* **75** 1169

[11] Lieberman M A and Lichtenberg A J 1971 *Phys. Rev.* A **5** 1852

[12] Pustilnikov L D 1983 *Theor. Math. Phys.* **57** 1035

Pustilnikov L D 1987 *Sov. Math. Dokl.* **35** 88

Pustilnikov L D 1995 *Russ. Acad. Sci. Sb. Math.* **82** 231

[13] Holmes P J 1982 *J. Sound Vib.* **84** 173

[14] Lichtenberg A J, Lieberman M A and Cohen R H 1980 *Physica* D **1** 291

[15] Karner G 1994 *J. Stat. Phys.* **77** 867

[16] Dembinski S T, Makowski A J and Peplowski P 1983 *Phys. Rev. Lett.* **70** 1093

[17] José J V and Cordery R 1986 *Phys. Rev. Lett.* **56** 290

[18] Seba P 1990 *Phys. Rev.* A **41** 2306

[19] Jain S R 1993 *Phys. Rev. Lett.* **70** 3553

[20] Leonel E D and McClintock P V E 2005 *J. Phys. A: Math. Gen.* **38** 823

[21] Tsang K Y and Lieberman M A 1984 *Phys. Lett.* A **103** 175

[22] Tsang K Y and Lieberman M A 1984 *Physica* D **11** 147

[23] Tsang K Y and Lieberman M A 1986 *Physica* D **21** 401

[24] Grebogi C, Ott E and Yorke J A 1982 *Phys. Rev. Lett.* **48** 1507

[25] Grebogi C, Ott E and Yorke J A 1983 *Physica* D **7** 181

[26] Kamphorst S O and de Carvalho S P 1999 *Nonlinearity* **12** 1363

[27] McDonald S W, Grebogi C, Ott E and Yorke J A 1985 *Phys. Lett.* A **107** 51

[28] Eckmann J P and Ruelle D 1985 *Rev. Mod. Phys.* **57** 617